Environmental Science & Technology

pubs.acs.org/est

Article

Transformation Products of Tire Rubber Antioxidant 6PPD in Heterogeneous Gas-Phase Ozonation: Identification and Environmental Occurrence

Haoqi Nina Zhao, Ximin Hu, Zhenyu Tian, Melissa Gonzalez, Craig A. Rideout, Katherine T. Peter, Michael C. Dodd,* and Edward P. Kolodziej*

Cite This: *Environ. Sci. Technol.* 2023, 57, 5621−5632

Read Online

ACCESS | Metrics & More | Article Recommendations | Supporting Information

ABSTRACT: 6PPD, a tire rubber antioxidant, poses substantial ecological risks because it can form a highly toxic quinone transformation product (TP), 6PPD-quinone (6PPDQ), during exposure to gas-phase ozone. Important data gaps exist regarding the structures, reaction mechanisms, and environmental occurrence of TPs from 6PPD ozonation. To address these data gaps, gas-phase ozonation of 6PPD was conducted over 24−168 h and ozonation TPs were characterized using high-resolution mass spectrometry. The probable structures were proposed for 23 TPs with 5 subsequently standard-verified. Consistent with prior findings, 6PPDQ ($C_{18}H_{22}N_2O_2$) was one of the major TPs in 6PPD ozonation (~1 to 19% yield). Notably, 6PPDQ was not observed during ozonation of 6QDI (*N*-(1,3-dimethylbutyl)-*N*′-phenyl-*p*-quinonediimine), indicating that 6PPDQ formation does not proceed through 6QDI or associated 6QDI TPs. Other major 6PPD TPs included multiple $C_{18}H_{22}N_2O$ and $C_{18}H_{22}N_2O_2$ isomers, with presumptive *N*-oxide, *N*,*N*′-dioxide, and orthoquinone structures. Standard-verified TPs were quantified in roadway-impacted environmental samples, with total concentrations of 130 ± 3.2 μg/g in methanol extracts of tire tread wear particles (TWPs), 34 ± 4 μg/g-TWP in aqueous TWP leachates, 2700 ± 1500 ng/L in roadway runoff, and 1900 ± 1200 ng/L in roadway-impacted creeks. These data demonstrate that 6PPD TPs are likely an important and ubiquitous class of contaminants in roadway-impacted environments.

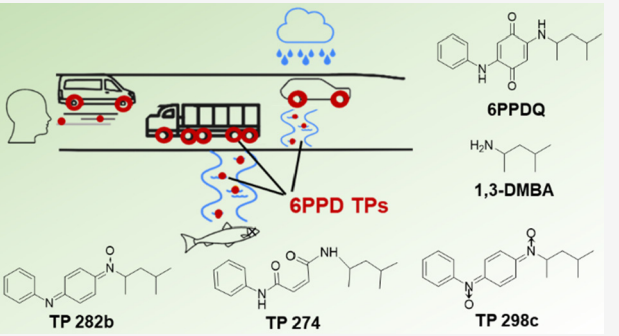

KEYWORDS: *6PPD, 6QDI, ozone, air, N-oxide, tire tread wear particles, roadway environments*

INTRODUCTION

Contaminants in stormwater and roadway runoff can adversely impact ecosystem health in receiving waters.[1−3] Stormwater toxicity has long focused on pollutants such as metals and polycyclic aromatic hydrocarbons, but these contaminants do not always explain observed adverse effects.[4,5] Therefore, characterizing unknown organic contaminants in roadway runoff, stormwater, and other non-point source pollution is an important research priority.[6−8]

Recently, our group identified 6PPD-quinone (6PPDQ), a highly toxic (LC_{50} for coho salmon, white-spotted char, and brook and rainbow trout: 95−1000 ng/L) ozone (O_3)-derived transformation product of 6PPD (*N*-(1,3-dimethylbutyl)-*N*′-phenyl-*p*-phenylenediamine);[9−13] 6PPDQ has now been detected globally in water,[14−22] dust,[23−27] and air samples.[28−32] 6PPD is ubiquitously used in tire rubbers as an antioxidant at 0.4−2% by weight,[33] where it is designed to quickly react with ground-level O_3 to protect rubber elastomers.[34,35] Such reactions inevitably form other transformation products (TPs) beyond 6PPDQ during the tire rubber lifetime.[21,34] For example, early studies on the antioxidant efficacy of 6PPD (e.g., Lattimer et al.) proposed several ozonation TPs based on low-resolution mass spectrometry and associated data.[34] Recently, using high-resolution mass spectrometry (HRMS), Klöckner et al. identified 6PPD-related chemical features as markers of tire and road wear particles,[36] and Hu et al. used gas-phase ozonation experiments to generate candidate feature lists for 6PPD TPs.[37] Seiwert et al. further reported 38 ozonation TPs of 6PPD from MS/MS structural information and screened their occurrence in snow and wastewater.[21] However, important uncertainties still exist regarding the environmental implications of 6PPD ozonation, including reaction mechanisms, especially the influence of oxygen and light; attaining high-confidence TP structures beyond tentative identification;

Received: November 18, 2022
Revised: February 5, 2023
Accepted: March 16, 2023
Published: March 30, 2023

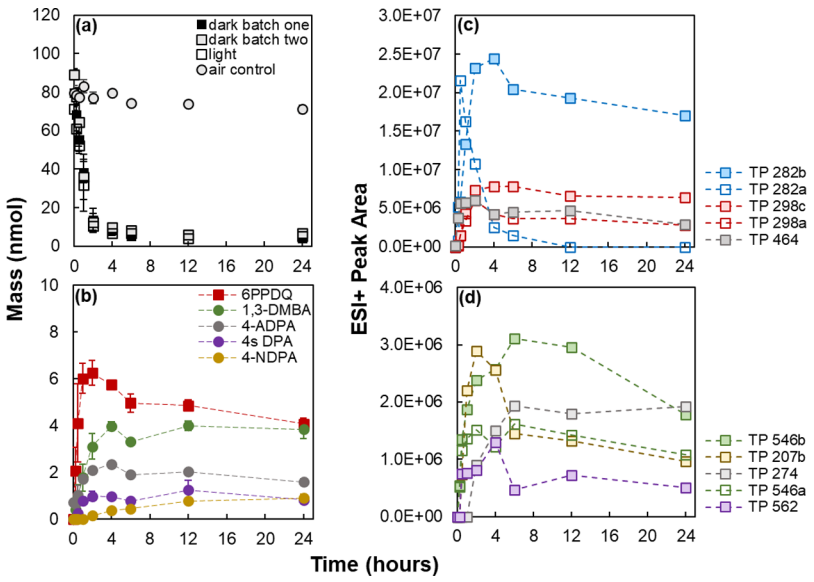

Figure 1. Time trends of 6PPD and detected TPs in gas phase ozonation. (a) Mass of 6PPD and (b) mass of level 1 TPs quantified with LC−MS/MS; (c) ESI+ peak areas of major TPs (with peak areas >1% of initial 6PPD peak area) without authentic standards; (d) ESI+ peak areas of some minor TPs (with peak areas <1% of initial 6PPD peak area) lacking authentic standards, including TP 274 and dimerization TPs. Peak areas of other minor 6PPD TPs not shown in this figure can be found in Figure S2. Panels (b), (c), and (d) show results from dark ozonation batch one. Symbols and error bars (shown for 6PPD and level 1 TPs in panels (a) and (b)) represent means and standard deviations of lab triplicates, respectively.

and quantification of these TPs in roadway-impacted environments. Considering their ubiquity and substantial mass discharge potential, rigorous characterization of 6PPD TPs and more broadly, the chemical mass balances of tire rubber-derived pollution, are urgent needs for environmental risk assessment.

In this study, we characterized TPs resulting from heterogeneous gas-phase ozonation of 6PPD. The reactions were performed in both the absence and presence of ambient room light with paired air controls (O_3-free compressed zero-grade air). Structures for the key TPs were proposed using HRMS (MS, MS/MS, and retention times (RTs) at different pH) supplemented by UV/vis spectroscopy data and confirmed with analytical standards when available. 6PPDQ formation pathways were also investigated through complementary ozonation experiments of *N*-(1,3-dimethylbutyl)-*N*′-phenyl-*p*-quinonediimine (6QDI), previously reported as an oxidation product of 6PPD and potential intermediate to 6PPDQ.[21,35,36] Tandem mass spectrometry (MS/MS) methods were then developed to quantify standard-confirmed TPs and qualitatively analyze two major TPs lacking authentic standards. Relevant TPs were screened and quantified in environmental samples relevant to roadways, including solvent extracts of O_3-exposed tire tread wear particles (TWPs) and solid phase extracts (SPE) of aqueous TWP leachate, roadway runoff, and roadway-impacted creeks.

MATERIALS AND METHODS

Chemicals. 6PPD was purchased as industrial grade (95% purity) from Usolf Chemicals (Shandong, China) and as analytical grade (98%) from Ambeed (Arlington Heights, IL, USA). 6QDI (solution in acetonitrile, 100 mg/L; 97%) was purchased from HPC Standards Inc (Atlanta, GA, USA). For TP standards (described as "level 1 TPs" throughout[38]), 6PPDQ (98.8%) was purchased from HPC Standards Inc; 4-nitrodiphenylamine (4-NDPA; 99%), 4-aminodiphenylamine (4-ADPA; 98%), and 1,3-dimethylbutylamine (1,3-DMBA; 98%) were from Sigma-Aldrich (St. Louis, MO, USA); 4-nitrosodiphenylamine (4s DPA) was from ChemService Inc. (West Chester, PA, USA), and 4-hydroxydiphenylamine (4-HDPA) was from Fisher Scientific (Pittsburgh, PA, USA). 6PPDQ-d_5 (solution in acetonitrile, 100 mg/L, full deuteration of the aniline ring) was purchased from HPC Standards Inc. All solid standards were stored in airtight bags (for industrial grade 6PPD; headspace evacuated) or bottles (for all other solid standards) at 4 °C. All dissolved standards were stored at −20 °C. OPTIMA grade acetone, methanol (MeOH), water, formic acid, and ammonium hydroxide solution (28−30%) were purchased from Fisher Scientific (Pittsburgh, PA, USA). Ammonium fluoride (>99.99%) was purchased from Sigma-Aldrich. For TPs lacking analytical standards, names are based on their molecular weight and relative order of liquid chromatography RTs among isomers (e.g., "TP 298a" refers to the first-eluting TP among 298 Da molecular weight isomers).

6PPD Ozonation. Exposure of 6PPD to gas-phase O_3 was first conducted in an ozonation chamber for 7 days (see Text S1, Figure S1). To reduce the dead volume and evaluate the rapidly-formed intermediate TPs, the chamber setup was replaced with a flow-through column (chamber: ∼30 × 20 × 20 cm, column, 2.5 × 20 cm) as performed by Hu et al. (Text S1, Figure S1).[37] Briefly, 6PPD-coated glass slides (4 × 2 cm; 2.5 μg 6PPD/cm^2) were ozonated (330 ± 6 ppbv) in triplicates in a glass column. O_3 exposures were conducted in series for 12, 0.25, 1, 4, 0.5, 2, 24, and 6 h (total run time ∼ 50 h); this exposure sequence was optimized based on instrument analysis speed to minimize sample holding time. TP formation was consistent between the chamber and column setups (Tables S1 and S2; Figures 1, S2, and S3); here, we largely report column ozonation results while using chamber data to assess long-term TP stability.

https://doi.org/10.1021/acs.est.2c08690
Environ. Sci. Technol. 2023, 57, 5621−5632

After ozone exposure in the column setup, 6PPD-coated slides were immediately extracted (10 mL MeOH, 30 min sonication) in amber glass bottles. 950 μL of the undiluted extracts were withdrawn, spiked with 50 μL of 100 μg/L 6PPDQ-d_5, and analyzed on an Agilent (Santa Clara, CA, USA) 1290 Infinity ultrahigh-performance LC system coupled to an Agilent 6530 quadrupole time-of-flight HRMS (LC-qTOF-HRMS) to screen for TPs. Additionally, 20 μL of undiluted, original extracts were withdrawn, brought to 1 mL with 930 μL of MeOH and 50 μL of 100 μg/L 6PPDQ-d_5 (50-fold dilution to bring analytes into instrument linear ranges), and analyzed on an Agilent 1290 Infinity UHPLC coupled to an Agilent 6460 triple quadrupole MS/MS (LC-MS/MS) to quantify 6PPD and 6PPDQ. Undiluted extracts were then analyzed directly on LC−MS/MS to quantify TPs with lower abundance. Instrumental analyses were completed within 48 h of sample collection with samples cooled at 4 °C on the autosampler during holding time.

O_3 exposures were undertaken twice under dark conditions (dark room; column wrapped with aluminum foil; experiments conducted under red light; described as "duplicate dark batches") and once under ambient room light (see Figure S4 for light spectra). 6PPD stocks and calibration curves were prepared freshly for each ozonation trial. Paired air controls (same column setup with 1 L/min O_3-free compressed zero-grade air (Airgas, Seattle, WA, USA)) evaluated potential 6PPD - oxygen reactions. Blank controls for O_3 and air column experiments were glass slides spiked with 20 μL of MeOH (n = 3 each column) that were exposed to 24 h of O_3 or air. No analytes were detected in blank controls except trace amounts of 6PPD (~0.02% of the 6PPD mass used for ozonation). Recovery controls were 6PPD-coated slides collected at t = 0 (prior to O_3 exposure) and showed recovery of 106 ± 5%.

Gas-phase O_3 exposure of 6QDI was conducted using a similar column apparatus to provide insights into potential 6PPDQ formation pathways. Notably, we detected large 6PPD signals when analyzing 6QDI commercial standards via LC-MS/MS. Complementary analyses, certificate of analysis, and manufacturer communications (HPC) indicated that 6PPD was not present within the 6QDI source stock as an impurity, but rather suggested conversion of 6QDI to 6PPD during LC−MS/MS analytical processes (Text S2). Due to resultant analytical uncertainties, 6QDI ozonation results were therefore considered qualitative.

TWP-Derived and Environmental Samples. To evaluate environmental relevance, 6PPD and six related level 1 TPs (five ozonation TPs: 6PPDQ, 1,3-DMBA, 4-ADPA, 4s DPA, and 4-NDPA; one reported aqueous reaction TP: 4-HDPA) were quantified in TWP solvent extracts (n = 3), TWP aqueous leachate (0.3 g TWP/L; n = 1, generated by circulating water through TWP-packed glass columns; triplicate extractions), roadway runoff (n = 4; grab sampled from two roads in two storm events; each with triplicate extractions), and roadway-impacted creek samples (Miller Creek in Burien, WA, USA; n = 5; 1 h composites at peak flows of five storm events from a roadway-impacted creek; each with single extraction) using LC−MS/MS. TP 282b (ozonation TP with the highest peak area) and TP 274 (ozonation TP previously observed with high peak areas in stormwaters)[39] were qualitatively screened, although they lacked analytical standards to enable quantification. To examine the effects of O_3 on 6PPD transformation and TP formation in tire rubber matrices, TWPs were exposed (6 h) to O_3 (360 ± 12 ppbv) or zero-grade air in triplicate glass columns (1 × 50 cm) under dark conditions, following Hu et al. (Text S3).[37] TWP samples were methanol-extracted, whereas TWP leachate, roadway runoff, and creek water samples were solid phase extracted; with triplicate lab blanks (i.e., empty extraction vials for TWPs; 200 mL DI water for aqueous samples) included for each extraction batch. Details of sample collection and processing are summarized in Text S3.

HRMS Analysis. LC-qTOF-HRMS analysis for TPs followed the methods described previously[39−41] (Text S4, Table S3). Briefly, full scan MS1 data were first acquired. Features were prioritized based on replicate and blank filters, followed by data-dependent MS/MS acquisition. Structures of potential TPs were inferred from the detected formula, RT and pH effects, diagnostic MS/MS neutral losses and fragments, and previous reports on 6PPD ozonation and transformation pathways (Text S4).[34,42] UV/vis spectra were acquired for selected TPs to aid structural diagnosis (methods in Text S5). Identification confidence was communicated following Schymanski et al:[38] level 1 identification was assigned to TPs when precursor mass, isotope pattern, RT, and MS/MS fragments matched the available commercial standards. Level 2a confidence represented TPs where MS/MS fragmentation, UV/vis absorbance features, and other diagnostic properties matched the literature, and level 2b reflected TPs where MS/MS information and known ozonation chemistry indicated a single structure. Level 3 described tentative structural candidates where MS/MS fragments matched plausible ozonation reactions, and specific reaction sites could (level 3a) or could not (level 3b) be assigned to molecular substructures. Level 4 described relevant molecular formula assignment without diagnostic MS/MS spectra.

LC−MS/MS Analysis. 6PPD and selected TPs were quantified (6PPD and level 1 TPs) or qualitatively screened (TP 282b, TP 274) in O_3-exposure samples, TWP extracts, and environmental samples using LC−MS/MS (Text S6, Table S4). 6QDI was qualitatively screened in O_3-exposure samples but not in TWP extracts or environmental samples. 6PPD and six level 1 TPs were quantified with 7-point calibration curves using 6PPDQ-d_5 as an internal standard (0.025−200 μg/L, R^2 > 0.995). Because analytes in TWP leachate and roadway runoff sometimes exceeded linear calibration ranges, these samples were diluted 10-fold post-extraction and re-injected to overcome detector saturation. The calculated concentrations were similar (<20% difference) in the undiluted and 10-fold diluted samples; therefore, concentrations in the diluted samples were reported but marked as semi-quantitative. For TWP-derived and environmental samples, 6PPD, 6PPDQ, 1,3-DMBA, 4-NDPA, and 4-HDPA were detected in lab blanks (Table S5); average lab blank concentrations were subtracted from the sample concentrations detected. Limits of detection (LODs) and quantification (LOQs) were defined as the average plus 3- and 10-fold standard deviations of lab blank concentrations, respectively, or as analyte concentrations with signal to noise ratios of 3 and 10, respectively, whichever were higher. LODs were 0.08−11 μg/g in TWP extracts, 0.18−30 ng/L in TWP leachate, 0.14−18 ng/L in roadway runoff, and 0.11−19 ng/L in creek samples. LOQs were 0.25−36 μg/g in TWP extracts, 0.59−70 ng/L in TWP leachate, 0.47−45 ng/L in roadway runoff, and 0.38−60 ng/L in creek samples. Concentrations between LODs and LOQs were marked as semi-quantitative.

https://doi.org/10.1021/acs.est.2c08690
Environ. Sci. Technol. 2023, 57, 5621−5632

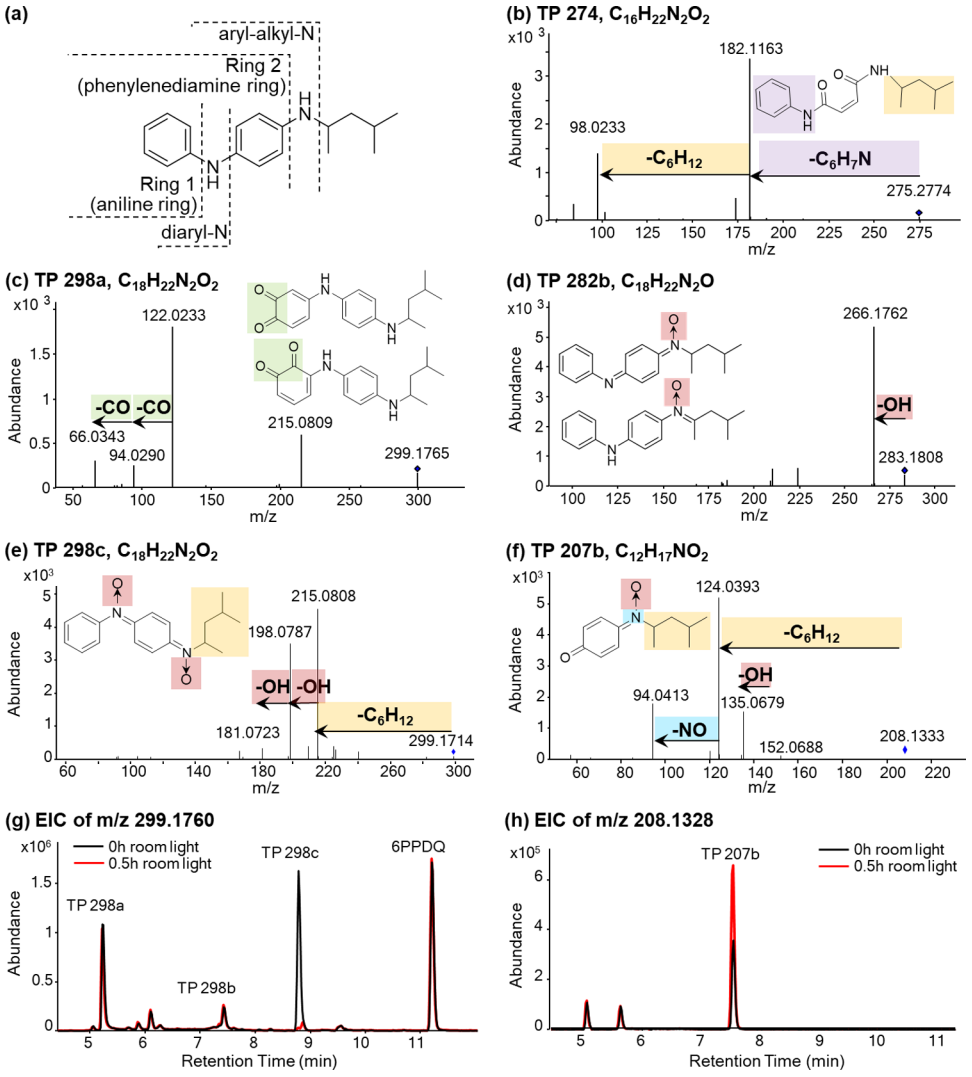

Figure 2. MS/MS spectra and ion chromatograms of select 6PPD TPs, including proposed structures. (a) Nomenclature of the ring structures and nitrogen atoms on 6PPD and related TPs. (b) MS/MS spectra of TP 274, (c) TP 298a, (d) TP 282b, (e) TP 298c, and (f) TP 207b. Diagnostic MS/MS neutral losses in the figure are matched with corresponding structural moieties by color-coded boxes. (g) Extracted ion chromatograms of TP 298 isomers and (h) TP 207b from samples of 6 h dark ozonated 6PPD subsequently subjected to either 0 h (black) or 0.5 h (red) of ambient room light exposure.

Spike recoveries of 6PPD and level 1 TPs were evaluated for TWPs, TWP leachate, roadway runoff, and creek samples in triplicate at concentrations close to the detected concentrations. Recoveries were defined as the detected concentrations in spiked samples (corrected for detection in unspiked samples) over nominal spike concentrations. Across the targeted analytes, recoveries ranged from 76 to 116% for TWPs, 79 to 133% for TWP leachate, 69 to 139% for roadway runoff, and 77 to 111% for creek samples (Table S5).

RESULTS AND DISCUSSION

6PPD Ozonation. In 6PPD-spiked recovery controls (6PPD spiked onto glass slides without exposure to O_3 or air), eight identified TPs were detected (4-ADPA, 1,3-DMBA, TP 312, TP 464, TP 280b, 4s DPA, 6PPDQ, and TP 282b; see Table S1 for TP peak areas; see Table S6 for all identified TP formulas and structures), reflecting impurities in the industrial-grade 6PPD standard or TP formation during 6PPD storage. The peak areas of detected TPs were <10% of the maximal peak areas in ozonated 6PPD extracts except 4-ADPA (19%). 6QDI was also detected in 6PPD recovery controls with an "apparent" peak area of 5% of 6PPD (see analytical uncertainty of 6QDI in Text S2).

No significant loss of 6PPD occurred in zero-grade air controls (p-value >0.05 in unpaired t test; Figure 1a), indicating that 6PPD was effectively inert to oxygen over the timescales investigated. The reaction kinetics of 6PPD in the duplicate dark ozonation batches and the ambient room light ozonation batch were not significantly different (p-value >0.05 in unpaired t test), indicating that room light had no significant effect on 6PPD transformation during ozone exposures. ~94% of the initial 6PPD mass (20 μg) reacted within 6 h; 12 and 24 h O_3 exposures did not significantly lead to further transformation of 6PPD (p-value >0.05 in unpaired t test; Figure 1a). Persistent residual 6PPD mass is consistent with past observations during exposure of 6PPD and other organic compounds to gas-phase O_3 at solid-air interfaces, where diffusion limitations or formation of protective surface films were suggested to limit penetration of O_3 to subsurface organic layers.[35,37,43−47] The same TPs were present in dark and light

https://doi.org/10.1021/acs.est.2c08690
Environ. Sci. Technol. 2023, 57, 5621−5632

ozonation experiments except TP 298c, which was only detected during dark ozonation (discussed below).

Transformation Product Identification. To identify TP structures, we integrated analytical data from (1) MS/MS spectra, (2) RTs under different mobile phase pH values, (3) UV/vis spectra from LC-photodiode array detector (DAD) analyses, and (4) literature MS/MS and UV/vis spectra data for similar compounds. For some TPs, MS/MS spectra were sufficient to propose a confident structure. For example, TP 274, observed at *m/z* 275.1753, has a molecular ion of $C_{16}H_{23}N_2O_2^+$. Characteristic fragments at *m/z* 182.1162 ($C_{10}H_{16}NO_2^+$, $-C_6H_7N$ from the molecular ion) and 98.0233 ($C_4H_4NO_2^+$, $-C_6H_{12}$ from *m/z* 182.1162) indicated an unreacted aniline ring (here called "Ring 1"; see nomenclature in Figure 2a) and an unreacted 1,3-dimethylbutyl group. Thus, TP 274 was a ring cleavage product of the phenylenediamine ring ("Ring 2" here), resulting from ozonolysis and elimination of two carbons. In addition, CO loss was observed at 40 eV (see full details of TP identification in Table S11). Based on plausible structures and reaction mechanisms, we propose an α,β-unsaturated dicarbonyl diamide structure for TP 274 (Level 2b, Figure 2b; Table S6).

When MS/MS spectra cannot resolve multiple structures, TP RTs can indicate functional group changes because of variations in hydrophobicity or pH effects on acid−base speciation of the amine, amide, and/or imine nitrogen. In general, the diaryl-*N* for possible 6PPD-derived TPs (predicted $pK_a < 0$) should remain neutral at analytically relevant pH, while ionization of the aryl-alkyl-*N* may vary depending on substitution or other modifications to the phenylenediamine ring (Table S7). Comparing relative RTs during HPLC analyses yields diagnostic insights because charged molecules elute faster than neutral molecules. For example, using acidic mobile phases, RTs of 6PPD (cationic, with predicted pK_a ~5.0 to 6.5 for the aryl-alkyl-*N*) and 6PPDQ (neutral, with predicted $pK_a < 0$ for the aryl-alkyl-*N*) were 6.9 and 11 min, respectively (Table S7). The much lower pK_a for 6PPDQ can be explained by the strong electron withdrawing effects of the neighboring quinone oxygens.[9]

An isomer of 6PPDQ, TP 298a (molecular ion of $C_{18}H_{23}N_2O_2^+$ at *m/z* 299.1754), had MS/MS spectra with diagnostic fragments of *m/z* 122.0227 ($C_6H_4NO_2^+$), 94.0294 ($C_5H_4NO^+$), and 66.0344 ($C_4H_4N^+$) that reflected consecutive losses of CO as characteristic MS/MS spectral features of *ortho*-quinones (Figure 2c).[48−50] Furthermore, the early RT (5.3 min) of TP 298a indicated an aryl-alkyl-*N* pK_a that was little affected by the incorporation of two oxygens into the 6PPD structure. Therefore, we propose a Ring 1 *ortho*-quinone structure for TP 298a (Level 2b, Table S6), which is supported by the predicted pK_a (3.8−6.4 for the aryl-alkyl-*N*; Table S7).

We also compared RTs of 6PPD ozonation TPs at different mobile phase pH (acidic (pH 2.8): 0.1% formic acid; circumneutral (pH 6.4): 1 mM ammonium fluoride; basic (pH 10): 0.1% ammonium hydroxide solution; same LC gradients and HRMS parameters). Two TP 282 isomers (*m/z* 283.1801, molecular ion of $C_{18}H_{23}N_2O^+$) were observed at 6.9 min (TP 282a) and 8.6 min (TP 282b) using acidic mobile phase. Both showed neutral loss of OH groups (fragmentation of *m/z* 283.1806−266.1761) that were reported as characteristic neutral losses for *N*-oxide structures (versus H_2O or O; Figure 2d).[51,52] However, the RT of TP 282a increased to 11.0 min in neutral and basic mobile phases, while the RT of TP 282b remained at 8.6 min. This indicated an ionizable aryl-alkyl-*N* for TP 282a but not for TP 282b; therefore, a diaryl-*N*-oxide structure is proposed for TP 282a and two possible aryl-alkyl-*N*-oxide structures for TP 282b (Table S6). The anticipated effects of the *N*-oxide position on RT are further supported by predicted log *D* values, which followed the order of TP 282a at pH 2.8 (log *D* = −1.32, 6.9 min RT) < TP 282b at all pH (log *D* = 2.17, 8.6 min RT) < TP 282a at pH 7 (log *D* = 3.56, 11.0 min RT; Table S7). The aryl-alkyl-*N*-oxide was previously proposed as an ozonation TP of 6PPD by Lattimer et al. (identified there as "6PPD nitrone").[34] Another possible structure for TP 282a could be a Ring 2 hydroxylated 6QDI (6QDI-OH),[21,36] although this structure is less consistent with the available MS2 spectral evidence (H_2O or O neutral loss is expected for 6QDI-OH). Further structural confirmation would need alternative analyses (e.g., NMR) or authentic standards.

For some structures, we performed additional characterization and proposed structures based on the literature-reported properties for analogous compounds. TP 298c (RT 8.7 min) had diagnostic fragments at *m/z* 215.0808 ($C_{12}H_{11}N_2O_2^+$), 198.0780 ($C_{12}H_{10}N_2O^+$), and 181.0749 ($C_{12}H_9N_2^+$), representing consecutive losses of OH groups and indicating an *N,N′*-dioxide structure (Figure 2e).[51,52] Notably, TP 298c was observed only under dark ozonation conditions. Furthermore, exposure of dark-ozonated (6 h) 6PPD (coated on glass slides) to room light for 0.5 h ($n = 3$) yielded complete decay of TP 298c (Figure 2g). Such sensitivity to light is consistent with *N,N′*-disubstituted *p*-quinonediimine-*N,N′*-dioxide structures.[53] According to prior reports, photodecay of the 6PPD *N,N′*-dioxide structure is anticipated to yield a *p*-quinoneimine-*N*-oxide TP retaining the aryl-alkyl-*N*.[53] Indeed, TP 207b was observed with the corresponding molecular formula ($C_{12}H_{17}NO_2$), and its MS/MS spectra supported the anticipated structure with OH neutral loss for *N*-oxide (Figure 2f). We also observed the TP 207b peak area to increase 2-fold in concert with TP 298c decay during 0.5 h of ambient room light exposure (Figure 2h). Finally, using LC-DAD, we observed a characteristic UV/vis absorbance maximum of 406 nm for TP 298c. This is consistent with the absorbance maxima (ranging from 385 to 435 nm) reported for numerous other *N,N′*-disubstituted *p*-quinonediimine-*N,N′*-dioxide structures.[54] The *N,N′*-dioxide also was proposed as a 6PPD ozonation TP in Lattimer et al. (there identified as "6PPD dinitrone").[34] Furthermore, "$C_{12}H_{17}NO_2$" was identified as a tire marker compound by Klöckner et al.[36] We thus propose TP 298c as the *N,N′*-dioxide of 6PPD and TP 207b as its corresponding *p*-quinoneimine-*N*-oxide TP at level 2a confidence.

Overall, twenty-five potential ozonation TPs were identified for 6PPD. Structures of relatively high confidence (level 1 or 2) were assigned for 9 TPs with five subsequently confirmed using analytical standards. Among the nine level 1 or 2 structures, three have been previously reported at level 1,[9,21,36,37] two were previously proposed at level 3 (by Lattimer et al. based on low-resolution mass spectrometry-derived molecular formula)[34] and are now reported with new UV/vis and HRMS structural information (especially for TP 298c as the *N,N′*-dioxide), and four were newly identified (1,3-DMBA, TP 207b, TP 298a, and TP 274) (Table S6). Probable structures (level 3a) were additionally proposed for 7 TPs (Table S6). Identification details are summarized in Table S11.

Ozonation Pathways. *N-Oxide and N,N′-Dioxide Formation.* Among the TPs identified, TP 282b and TP 282a

https://doi.org/10.1021/acs.est.2c08690
Environ. Sci. Technol. 2023, 57, 5621−5632

were most abundantly observed (ESI+ peak areas) across all time points (Figure 1c). TP 282b, proposed as an aryl-alkyl-*N*-oxide, was a metastable TP that accumulated over 4 h of ozonation and subsequently decreased (~30% peak area loss from 4 to 24 h). In contrast, TP 282a, the potential diaryl-*N*-oxide, formed over 0.5 h and appeared to quickly transform further (~90% peak area decrease by 4 h; Figure 1c). This was consistent with Lattimer et al. reporting an aryl-alkyl-*N*-oxide (i.e., "6PPD nitrone") as a dominant TP during longer term (500 ppb O_3 for one week) gas-phase ozonation of 6PPD.[34] The proposed *N*-oxide formation pathway was through O_3 addition to aryl-alkyl-*N*, yielding a nitroxide radical intermediate, which then formed the *N*-oxide product via $H^{\bullet}$ loss and reaction with another O_3 to yield *N*,*N*′-dioxide.[34] Correspondingly, TP 298c, likely, the *N*,*N*′-dioxide, had the fourth largest ESI+ peak areas among all TPs during dark ozonation and seemed more stable than either TP282a or TP 282b to O_3, with a maximal peak area at 4 h and 17% subsequent loss by 24 h (Figure 1c). On this basis, we tentatively propose both TP282a, the likely diaryl-*N*-oxide, and TP282b, likely an aryl-alkyl-*N*-oxide with one of two possible structures (Table S6), as potential intermediates to TP298c. Further characterization (e.g., isolation and NMR) would help confirm these pathways.

6PPDQ Formation. 6PPDQ (TP 298d, level 1) was observed with the third largest ESI+ peak area and appeared to be metastable. Via LC−MS/MS quantification, 6PPDQ mass peaked at 2 h of O_3 exposure and 35% of this mass reacted away by 24 h (Figure 1b), consistent with recent observations of 6PPDQ ozonation.[21] The average molar yields of 6PPDQ from 6PPD were 10 ± 5% across all time points with a maximum 19% yield observed at 0.5 h (Table S6), consistent with the ~9.7% molar yield we recently reported for an independent series of gas-phase ozonation experiments.[37] We previously suggested 6PPDQ formation through initial O_3 addition to 6PPD's Ring 2 at one of the positions *ortho*- to the two N atoms, forming either a hydroxy 6PPD intermediate or a 6PPD semiquinone radical intermediate.[9] Recently, Seiwert et al. and Klöckner et al. proposed another 6PPDQ formation pathway proceeding through 6QDI and 6QDI-OH.[21,36] Our observations here are more consistent with pathways involving the hydroxy or semiquinone intermediates, considering that (1) these pathways conform with the *ortho*−/*para*-directing resonance character of electron-donating substituents (i.e., amino and hydroxy groups) in oxidation reactions of activated aromatic compounds and with the reported reaction mechanisms for analogous phenols and anilines;[9,55−57] (2) 6QDI formation was not observed here during 6PPD ozonation (rather, the peak area of 6QDI initially present as an impurity in 6PPD stocks decreased by 90% in 0.25 h 6PPD ozonation; Table S1); and (3) in additional experiments investigating direct exposure of 6QDI to gas-phase O_3, 6PPDQ was not detected (Figure S5).

TP 298a, observed with the fifth largest ESI+ peak areas, may form through similar pathways as 6PPDQ but with O_3 reaction on 6PPD Ring 1. Initial O_3 attack at one of the positions *ortho*- or *para*- to the diaryl-*N*, followed by secondary oxygen addition *ortho*- to the first site of O_3 attack, could thereby yield a 2,3-*ortho*-quinone or 3,4-*ortho*-quinone structure, respectively (Table S6).

Oxidative Coupling. Consistent with oxidative coupling, apparent dimerization products of 6PPD were observed with relatively large peak areas (Figure 1c,d). These include TP 464 ($C_{30}H_{42}N_4O$; the sixth most abundant TP), TP 546a/b ($C_{36}H_{42}N_4O$), and TP 562 ($C_{36}H_{42}N_4O_2$). Dimerization of 6PPD was previously reported during gas-phase O_3 exposure via formation of diaryl-*N* radicals;[34] the aromatic substituents sufficiently stabilize the diaryl-*N* radical intermediate to allow oxidative coupling. Here, TP464 likely reflects a secondary oxidative TP after coupling of 6PPD and 4-ADPA, while TP 546 and TP 562 likely reflect secondary oxidative TPs of the 6PPD dimer (Table S6). While dimer formation may be an artifact of the elevated 6PPD concentrations in gas-phase ozonation, we anticipate especially low solubility for these larger MW products. Notably, 6PPD polymerization reactions have been implicated in protection effects on tire surfaces;[35,37,43−47] the environmental relevance of dimeric or polymeric TPs for surface environments merits further investigation.

TP 274. Notably, TP 274 formation was observed in both 6PPD and 6QDI ozonation. The peak area ratios of TP 274 relative to initial 6QDI were quite similar in 6PPD and 6QDI ozonation (Text S2, Tables S1 and S8), suggesting that TP 274 observed in 6PPD ozonation plausibly originated from the 6QDI impurity present in the 6PPD standard. It was not possible to further test this hypothesis with 6QDI-free 6PPD because we detected 6QDI in every 6PPD standard we purchased. TP 274 is also an environmentally notable TP. It exhibited high peak area growth in ozonated TWPs, and it was commonly and abundantly detected in environmental samples (see Figure 4). It was also previously identified by Peter et al. (as a *m*/*z* 333.2212 adduct) within the "toxicant signature" of coho salmon mortality events and by Klöckner et al. (as a HRMS feature with the $C_{16}H_{22}N_2O_2$ formula) as a stable tire marker.[36,39] The *α*,*β*-unsaturated dicarbonyl diamide structure proposed for TP 274 is similar to TPs observed in aqueous ozonation of phenols and furans,[55,58,59] some of which are reactive with lysine and cysteine groups and capable of protein damage.[58,60]

4-ADPA, 4s DPA, and 4-NDPA. 4-Nitrosodiphenylamine (4s DPA; $C_{12}H_{10}N_2O$) was the seventh most abundant TP based on ESI+ peak area and was standard-confirmed (Table S6). 4s DPA molar mass increased rapidly over 2 h of ozonation (maximum molar yield 1.5% through LC−MS/MS quantification) and remained stable from 2 to 24 h (Figure 1b). As suggested previously,[21,34] 4s DPA could form directly from 6PPD via successive steps of oxygen transfer and oxidation by O_3 at the electron rich aryl-alkyl-*N*.[34] Alternatively, 4s DPA could be the oxidation product of 4-aminodiphenylamine (ADPA; $C_{12}H_{12}N_2$), another standard-confirmed TP of 6PPD reported to form through an *α*-carbon hydroxy intermediate.[21] The second pathway is consistent with the observed metastability of 4-ADPA, which accumulated over 4 h (maximum molar yield 2.1%), then decayed (33% mass lost) over 4−24 h. Further oxidation of 4s DPA could then lead to standard-confirmed 4-NDPA ($C_{12}H_{10}N_2O_2$) as a stable terminal product;[34] 4-NDPA showed continuous accumulation during 24 h ozonation with a maximum molar yield of 1.1% (Figure 1b, Table S6).

1,3-DMBA. Standard-confirmed 1,3-dimethylbutylamine (1,3-DMBA) also formed during 6PPD ozonation. 1,3-DMBA molar yields were stable with time and averaged 4.2 ± 0.5% (Table S6). 1,3-DMBA was previously reported as a hydrolysis product of 6PPD.[42] In this case, 1,3-DMBA more likely arises through oxidative reactions, potentially through a

https://doi.org/10.1021/acs.est.2c08690
Environ. Sci. Technol. 2023, 57, 5621−5632

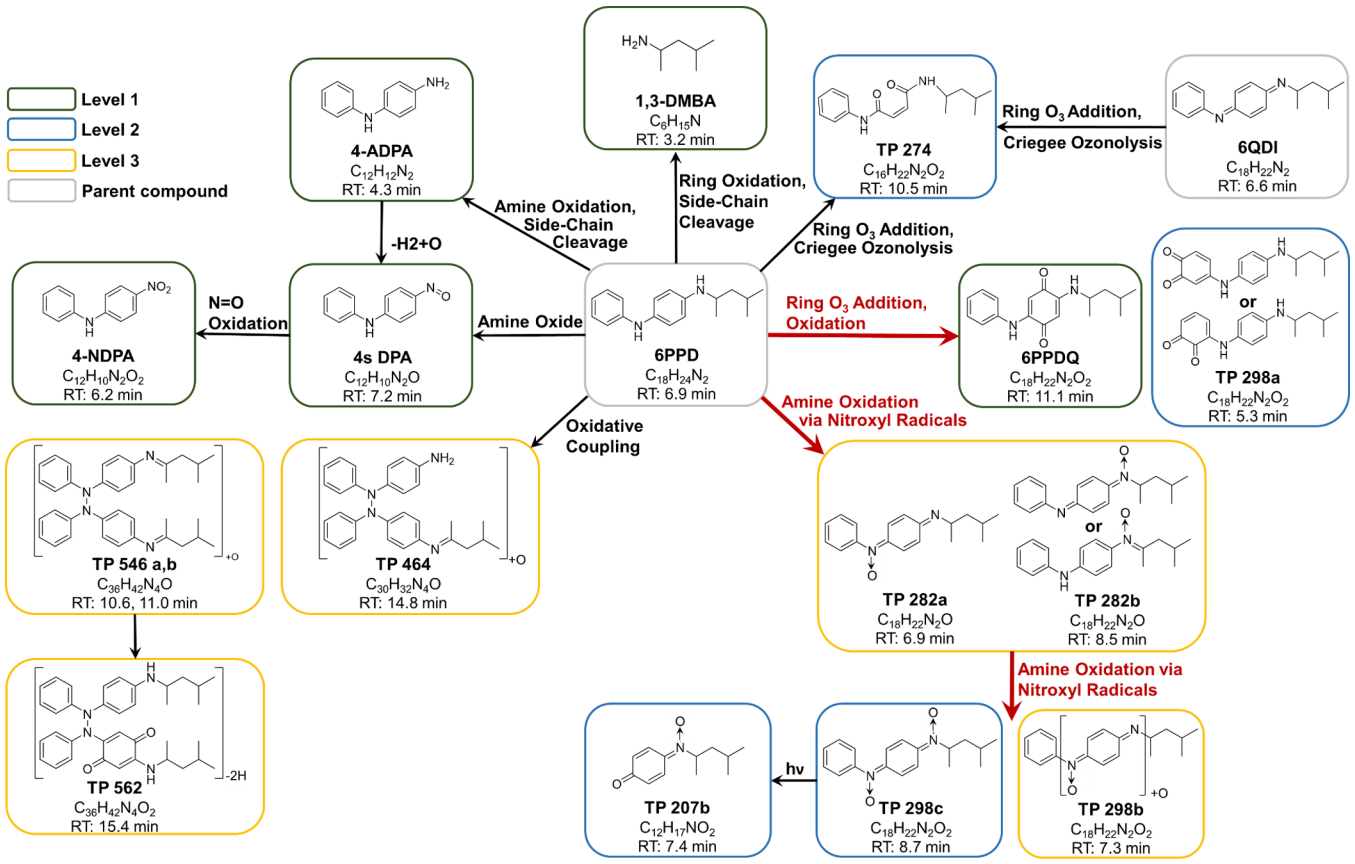

Figure 3. Proposed ozonation pathways for 6PPD along with chemical formulas, retention times (RT), and proposed structures for detected TPs. TP structures identified with confidence levels 1, 2, and 3 are indicated by green, blue, and yellow boxes, respectively. Parent 6PPD and 6QDI structures are in gray boxes. Major pathways (based on TP ESI+ peak areas) are highlighted with red arrows. While 6QDI has been reported as an oxidation product of 6PPD via reaction with O_2 or O_3,[21,35,36] clear evidence of formation during 6PPD ozonation was not observed in this study.

Table 1. Detection Frequencies (DF) and Concentrations of 6PPD and Related TPs in TWP Methanolic Extracts (before and after TWP Ozonation, n = 3), TWP Leachate (0.3 g TWP/L; n = 1 with Triplicate Extraction), Roadway Runoff (n = 4 with Triplicate Extraction), and Roadway-impacted Creek Samples (n = 5 with Single Extraction)[a]

		TWP extract (μg/g TWP)			TWP leachate (μg/g TWP)	Roadway runoff (ng/L)		Roadway-impacted creek (ng/L)	
		pre-ozonated	air control	ozonated		DF	Concentration	DF	Concentration
concentration	6PPD	1500 ± 40	1500 ± 200	610 ± 20	4.7 ± 0.2[b,c]	4/4	75 ± 40[c]	5/5	99 ± 64[c]
	6PPDQ	12 ± 0.2	13 ± 1	26 ± 2	1.6 ± 0.03	4/4	140 ± 60	5/5	90 ± 20
	1,3-DMBA	70 ± 2	76 ± 10	88 ± 4	25 ± 3[b]	4/4	2200 ± 1200[b]	5/5	1400 ± 900[b]
	4-HDPA	29 ± 1	30 ± 4	31 ± 3	7.0 ± 0.7[b]	4/4	150 ± 100	5/5	110 ± 50
	4-ADPA	14 ± 0.6	14 ± 2	36 ± 3	0.33 ± 0.02	2/4[d]	110 ± 110	4/5[d]	140 ± 100
	4s DPA	<LOD	<LOD	15 ± 3	0.31 ± 0.02	4/4	100 ± 50	5/5	180 ± 110
	4-NDPA	1.2 ± 0.01	1.4 ± 0.1	2.3 ± 0.2	0.26 ± 0.01	4/4	21 ± 15	5/5	8.3 ± 2.5
	ΣTPs[d]	130 ± 3.2	130 ± 20	200 ± 20	34 ± 4		2700 ± 1500		1900 ± 1200
peak area ratios to 6PPDQ	TP 274	4.5 ± 0.4	4.1 ± 0.2	9.0 ± 0.1	19 ± 0.3	4/4	68 ± 35	5/5	66 ± 30
	TP 282b	0.2 ± 0.002	0.22 ± 0.08	8.7 ± 0.6	3.5 ± 0.6	4/4	40 ± 12	5/5	65 ± 15

[a]Lacking commercial standards, TP 274 and TP 282b were assessed by their LC−MS/MS peak area ratios relative to 6PPDQ (TP 274 transition: 275.1 to 182.1, TP 282b transition: 283.2 to 266.1, and 6PPDQ transition 299.2 to 215.1). [b]Concentrations were considered semi-quantitative due to the detected concentrations exceeding the calibration ranges. [c]6PPD concentrations are considered semi-quantitative due to its potential instability in aqueous solution. [d]Values <LODs were replaced by 0 in sum calculation.

similar pathway as 4-ADPA, except with C−N cleavage between the aryl-alkyl-N and Ring 2.

Based on the above-identified and probable structures, tentative ozonation pathways for 6PPD are proposed in Figure 3.

Tire Wear Particles. To investigate the environmental discharge of the identified 6PPD TPs, we first screened TWP methanolic extracts and TWP aqueous leachate. We quantified 6PPD, five level 1 ozonation TPs (including 6PPDQ), and 4-HDPA, the major 6PPD aqueous reaction product (Table S6), with LC−MS/MS and internal standard (6PPDQ-d_5) calibration. Additionally, we qualitatively detected TP 282b and TP 274 using LC−MS/MS transitions developed with 6PPD ozonation mixtures. Notably, environmental 6PPD TPs

https://doi.org/10.1021/acs.est.2c08690
Environ. Sci. Technol. 2023, 57, 5621−5632

may form either in gas-phase reactions (during tire manufacture, product use, and after TWPs release) or aqueous-phase reactions (after 6PPD leaching into the aquatic environment from TWPs). Although we only identified TPs in gas-phase ozonation, we expect similar TPs to form in aqueous ozonation because Seiwert et al. observed similar reaction pathways for gas- and aqueous-phase ozonation of 6PPD.[21] The analysis of TWP methanolic extracts reflected gas-phase reactions, while the TWP aqueous leachate potentially reflected both gas- and aqueous-phase reactions during the 8 h leaching time.

TWP Extracts. 6PPD dominated the detected chemical mass in pre-ozonation, solvent-extracted TWPs (1500 ± 40 μg/g TWP) (Table 1). The detected 6PPD is lower than the reported mass ratios (0.4−2%) in new rubber,[33] which may reflect the use of both new and used (i.e. 6PPD-depleted) tires in this TWP mixture and non-exhaustive (spike recovery: 76 ± 1%) extraction methods focused on surficial mass. 6PPD was reported in tire and road wear particles (TRWPs) at 1000 ± 630 μg/g TRWP.[61] Assuming equal mass of the tread polymer and road encrustations in TRWPs,[62] 6PPD concentrations in our TWP mixture are quite similar to those reported for the TRWP tread polymer (~2000 ± 1260 μg/g TRWP tread polymer). All targeted TPs (level 1 TPs, TP 282b, and TP 274) were detected in pre-ozonation TWPs except 4s DPA (Table 1), likely reflecting used tire compositions and/or TP generation during TWP storage. The ΣTPs (130 ± 3.2 μg/g) were dominated by 1,3-DMBA (70 ± 2 μg/g TWP; 55% contribution), with large contributions from 4-HDPA (29 ± 1 μg/g TWP; 23%), 4-ADPA (14 ± 0.6 μg/g TWP; 11%), and 6PPDQ (12 ± 0.2 μg/g TWP; 10%; Figure 4). 4-HDPA (42 ± 33 μg/g TRWP) and 4-ADPA (17 ± 25 μg/g TRWP) were previously reported in TRWPs. The equivalent concentrations reported for tread polymer (4-HDPA, 84 ± 66 μg/g TRWP tread polymer; 4-ADPA, 34 ± 50 μg/g TRWP tread polymer) were ~2-fold higher than those in our TWP mixture.[61] Different tire formulations or extraction methods (Soxhlet versus sonication) also may explain such compositional differences.

After 6 h of dark O_3 exposure, 59% of detected 6PPD in TWPs had reacted and the ΣTPs concentrations increased ~1.5 fold (p-value <0.05 in unpaired t-test; Table 1, Figure 4a). 6PPD and ΣTPs concentrations were unchanged during exposure to zero-grade air (p-value >0.05 in unpaired t-test), confirming the critical role of O_3 in TP formation at these time scales (Table 1, Figure 4a). Molar yields (mole TP formed per mole 6PPD reacted) for TWP ozonation were highest for 1,3-DMBA (5.5 ± 0.9%), followed by 4-ADPA (3.6 ± 0.4%), 4s DPA (2.2 ± 0.3%), 6PPDQ (1.4 ± 0.2%), and 4-NDPA (0.15 ± 0.2%). Compared with pure phase 6PPD ozonation, the yields of 6PPDQ and 4-NDPA in TWP ozonation were lower and the yields for other TPs were higher (Table S6), indicating that the TWP matrix and surface effects affected ozonation mechanisms or kinetics. Notably, while the ESI+ HRMS peak area of TP 274 was relatively low in pure phase 6PPD ozonation (e.g., ~20% that of 6PPDQ), TP 274 exhibited large LC−MS/MS peak areas in both TWP pre- and post-ozonation extracts. The peak area of the quantifier LC−MS/MS transition of TP 274 was ~4.5 times that of 6PPDQ in TWP pre-ozonation; this ratio increased to 9.0 post-ozonation (Table 1, Figure 4d). Although complicated by the potentially large difference in peak area response, TP 274 seems present in TWP matrices at levels similar to or higher than 6PPDQ. For

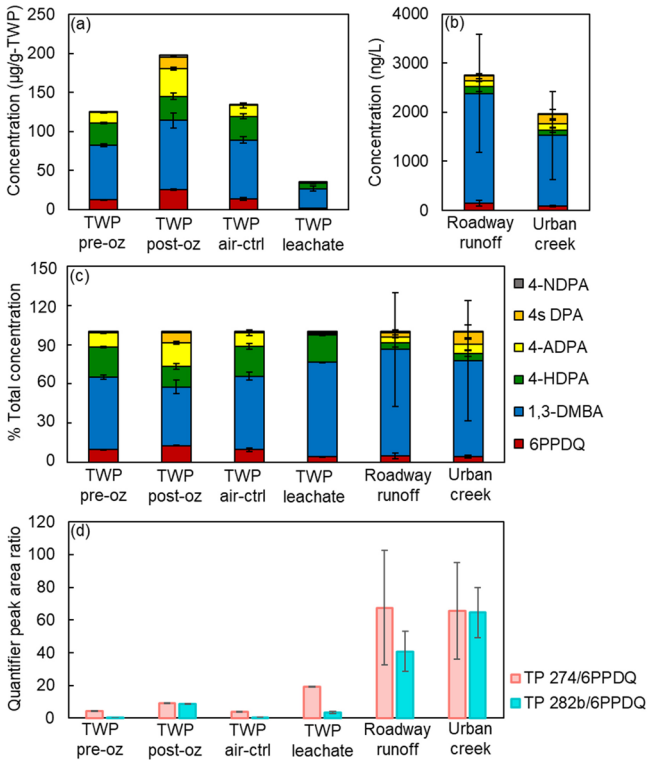

Figure 4. Detection of the targeted TPs in TWP-derived and environmental samples. (a) Concentrations of level 1 TPs in TWP solvent extracts (before ozonation "pre-oz"; after 6 h ozonation "post-oz"; air control "air ctrl"; n = 3) and TWP leachate (0.3 g TWP/L; n = 1 with triplicate extraction); (b) Concentrations of level 1 TPs in roadway runoff (n = 4 with triplicate extraction) and roadway-impacted creek samples (n = 5 with single extraction); (c) Relative contributions of individual TPs to ΣTP concentrations in different matrixes; (d) Peak area ratios of the LC−MS/MS quantifier transitions of TP 274 and TP 282b over that of 6PPDQ. Values below LODs were estimated as 0.

TP 282b, its peak area ratio with 6PPDQ was 0.2 in pre-ozonation TWPs and increased to 8.7 post-ozonation (Figure 4d). This is consistent with pure phase 6PPD ozonation, where TP 282b was the most abundant TP.

TWP Leachate. 6PPD was detected in TWP leachate (Table 1). Although we semi-quantified it at 4.7 ± 0.2 μg/g TWP equivalent, 6PPD concentrations in aqueous systems should generally be treated cautiously, given its reported instability in water that can result in low-biased concentrations.[42] After all, the antioxidant 6PPD is designed to react, with clear implications for its analytical stability and accurate quantification. All targeted TPs were detected in TWP leachate. Compared with TWP extracts, the contributions of 1,3-DMBA (25 ± 3 μg/g TWP; 72% contribution) and 4-HDPA (7.0 ± 0.7 μg/g TWP; 21% contribution) to ΣTPs further increased, followed by 5% contribution from 6PPDQ (1.6 ± 0.03 μg/g TWP) and <1% contribution from 4-ADPA, 4s DPA, and 4-NDPA (Table 1, Figure 4). 1,3-DMBA and 4-HDPA are major TPs of 6PPD decay in water;[42] their increased ΣTPs contributions likely reflect aqueous transformation reactions of residual 6PPD and its TPs in leachates. In previous TRWP column leaching tests, Unice et al. and Klöckner et al. reported the absence of 4-ADPA, 4-HDPA, 4-NDPA, and 6PPDQ in aqueous leachate of TRWP.[36,61] Both studies used ionic solutions (0.001 M $CaCl_2$ in Unice et al.; 0.2

https://doi.org/10.1021/acs.est.2c08690
Environ. Sci. Technol. 2023, 57, 5621−5632

M phosphate buffer in Klöckner et al.) for leaching (compared to DI water here) and did not employ sample enrichment (versus 200-fold SPE extraction here),[36,61] which may result in reduced leaching potentials for cationic TPs, higher LODs, or ion suppression during mass spectrometry. Also, Klöckner et al. used syringe filtration (0.45 μm cellulose acetate) to separate TWPs from solution, which may result in sorptive losses of 6PPDQ and other TPs to filter materials. These factors likely contribute to disparate observations across similar systems.

The observed peak area ratios of TP 274/6PPDQ and TP 282b/6PPDQ increased to 19 and 3.5 in TWP leachate, respectively, from 4.5 and 0.2 in TWP methanolic extract (Figure 4d). This may reflect favorable TP 274 and TP 282b partitioning from tire rubber to water compared to 6PPDQ, which is consistent with the lower log D values predicted for TP 274 and TP 282b (ChemAxon log D: TP 274, 2.84; TP 282b, 2.17; 6PPDQ, 3.24; Table S7).

Environmental Occurrence. To verify environmental relevance of these TPs, we analyzed several roadway runoff and roadway-impacted creek samples collected in fall 2021 for the same TPs as in TWP samples (level 1 ozonation TPs, 4-HDPA, TP 282b, and TP 274). 6PPD was detected in all runoff samples (4/4; semi-quantitatively at ~75 ± 40 ng/L). For TPs, all targeted TPs except 4-ADPA (2/4 detection) were detected in all roadway runoff samples. Similar to TWP leachate, the ΣTPs (2700 ± 1500 ng/L) were dominated by 1,3-DMBA (2200 ± 1200 ng/L, 81% contribution; Figure 4). However, 4-HDPA, the second most abundant TP in TWP leachate, had lower concentrations in this roadway runoff (150 ± 100 ng/L; 5% contribution) that suggested environmental instability (e.g., photo-transformation half-life of 4-HDPA reported as 1.3 h).[42] 6PPDQ (140 ± 60 ng/L), 4-ADPA (110 ± 110 ng/L), and 4s DPA (100 ± 50 ng/L) all showed ~5% contributions to total ΣTPs (Figure 4). The increased contributions of 4s DPA and 4-ADPA in roadway runoff may suggest additional environmental sources beyond TWP. For example, 4-ADPA is used as an antioxidant or precursor in fuels and lubricants.[63] 4s DPA is a chemical intermediate for dyes and pharmaceuticals and also used as a polymerization inhibitor during vinyl production.[64] Therefore, 4-ADPA and 4s DPA are examples of industrial TPs whose formation and environmental occurrence can arise via multiple sources other than 6PPD. For 1,3-DMBA (a small aliphatic amine), although its high abundance in TWPs correlates well with its high environmental occurrence, we still note that there are potential sources of 1,3-DMBA other than as a 6PPD TP.[65] For example, it is reported as a potent stimulant used in dietary supplements.[66,67] TP 274/6PPDQ and TP 282b/6PPDQ peak area ratios were increased to 68 and 40 in roadway runoff versus 19 and 3 in TWP leachate, respectively (Figure 4d). The abundance and stability of TP 274 in TWP leachate and roadway runoff similarly indicate its high potential for environmental discharge; we now consider TP 274 to be a major environmentally relevant TP of 6PPD. Although lack of analytical standards precluded its quantification here, TP 274 merits full characterization. Measured 6PPDQ concentrations in runoff samples (140 ± 60 ng/L) were relatively low; possibly because this roadway was not heavily trafficked, compared with prior reports addressing roadway runoff from Seattle and Los Angeles (54−1300 ng/L),[11] stormwater collected from Canada (35−627 ng/L),[14,18] and runoff collected in China (210−2430 ng/L).[68]

6PPD was detected in the roadway-impacted creek (Miller Creek) in all storm events (5/5, semi-quantitatively at 99 ± 64 ng/L). Except for 4-ADPA (4/5 detection), all targeted TPs were also detected in all storm events. The ΣTPs (1900 ± 1200 ng/L) was again dominated by 1,3-DMBA (1400 ± 900 ng/L, 73% contribution), followed by 4s DPA (180 ± 110 ng/L, 9%), 4-ADPA (140 ± 110 ng/L, 7%), 4-HDPA (110 ± 50 ng/L, 6%), 6PPDQ (90 ± 20 ng/L, 5%), and 4-NDPA (8.3 ± 2.5 ng/L, 0.4%; Table 1, Figure 4). Except for a slight increase in 4s DPA (2.5-fold) and 4-ADPA contributions (1.8-fold), TP compositions, including the peak area ratios of TP 274/6PPDQ and TP 282b/6PPDQ, were very similar between roadway runoff and roadway-impacted creeks (<1.2-fold variance), indicating roadway runoff as the major source of TPs in receiving waters during storms. This could happen either through direct discharge of the TPs, or transport of TWPs into receiving waters coupled with further chemical leaching and in situ aqueous-phase ozone exposure. Measured 6PPDQ concentrations in this roadway-impacted creek (90 ± 20 ng/L) during storm events were consistent with recent global reports, addressing receiving waters in Seattle and San Francisco (19−230 ng/L),[11] a runoff-receiving tributary in Australia (88 ng/L at the storm peak),[19] runoff-receiving rivers from Toronto, Canada (110−720 ng/L),[22] snowmelt from Saskatoon Canada (80−370 ng/L),[14] and wastewater treatment plant influents receiving snowmelt (105 ng/L) and rainfall (52 ng/L) in Germany.[21] We note that in fall 2021, 68% of adult coho salmon returning to Miller Creek perished from urban runoff mortality syndrome (personal communication, Iris Kemp, King County, WA, USA), consistent with our recent estimate of 95 ng/L for the 6PPDQ LC_{50}.[11]

Overall, these data demonstrated the discharge of 6PPD-derived TPs into aquatic environments through leaching of tire rubbers during wet periods. 1,3-DMBA, TP 274, TP 282b, and 6PPDQ appear to be the most environmentally relevant TPs in terms of their occurrence and/or toxicity.[11] As individual contaminants, these 6PPD TPs are quite abundant (frequently detected and can be present at μg/L concentrations) in roadway runoff and associated receiving waters relative to many other roadway-derived contaminants.[3] For example, 1,3-diphenylguanidine, a widely used tire vulcanization accelerator, was detected in stormwater samples from the same watershed at 5.4−540 ng/L[69] and in European surface waters at <LOD-170 ng/L.[70] Methyl-1H-benzotriazole, used as a corrosion inhibitor, was detected at up to 5600 ng/L in stormwater runoff.[1] Hexa(methoxymethyl)melamine (HMMM), used in part for tire manufacture,[71] was detected at ~1700 ng/L in stormwater-impacted receiving waters in Canada,[72] at 5000 ng/L (including 12 TPs) in European surface water,[73] <LOD-280 ng/L in Australian surface waters,[74] and up to 1500 ng/L in fall 2018 stormwaters in the same watershed as the samples included here.[75] Based on roadway runoff concentrations (ΣTPs, 2700 ± 1500 ng/L; Table 1), the environmental load of these 6PPD TPs in the US is potentially as high as 92,000 ± 51,000 kg/year (U.S highway length, 14,200,000 km;[76] lane width, 3.7 meters;[76] average precipitation rate, 769 mm/year;[77] runoff coefficient, 0.85[78]). While the concentration estimates reported here do not yet employ more accurate isotope dilution methodologies for each compound (6PPDQ-d_5 used as the internal standard for all targets), these data clearly indicate that 6PPD ozonation TPs, including 6PPDQ and others, are an important and likely ubiquitous class of emerging contaminants in roadway-impacted environments.

https://doi.org/10.1021/acs.est.2c08690
Environ. Sci. Technol. 2023, 57, 5621−5632

■ ASSOCIATED CONTENT

Supporting Information

The Supporting Information is available free of charge at https://pubs.acs.org/doi/10.1021/acs.est.2c08690.

6PPD ozonation setup; 6QDI ozonation setup and results; TWPs and environmental sample collection and processing; instrumental methods of HRMS; UV/vis spectroscopy; LC−MS/MS analysis; schematic diagrams of the ozonation systems; 6PPD TP time trends in column and chamber ozonation; emission spectra of the red light and ambient room light; extracted ion chromatograms of 6PPDQ in 6QDI ozonation; chromatograms showing interchange of 6PPD and 6QDI in LC−MS analysis; TP LC-qTOF-HRMS peak areas in 6PPD column and chamber ozonation; HRMS feature extraction and alignment parameters; LC−MS/MS dMRM parameters; quality assurance and quality control data; TP formulas and structures; predicted log D and pK_a values; TP peak areas in 6QDI ozonation; 6PPD and 6QDI peak areas in semi-direct standard injection; TP concentrations in individual environmental samples; and TP identification details (PDF)

■ AUTHOR INFORMATION

Corresponding Authors

Michael C. Dodd − *Department of Civil and Environmental Engineering, University of Washington, Seattle, Washington 98195, United States*; Email: doddm@uw.edu

Edward P. Kolodziej − *Department of Civil and Environmental Engineering, University of Washington, Seattle, Washington 98195, United States; Center for Urban Waters, Tacoma, Washington 98421, United States; Interdisciplinary Arts and Sciences, University of Washington Tacoma, Tacoma, Washington 98421, United States;* orcid.org/0000-0002-7968-4198; Email: koloj@uw.edu

Authors

Haoqi Nina Zhao − *Department of Civil and Environmental Engineering, University of Washington, Seattle, Washington 98195, United States; Center for Urban Waters, Tacoma, Washington 98421, United States;* orcid.org/0000-0003-3908-630X

Ximin Hu − *Department of Civil and Environmental Engineering, University of Washington, Seattle, Washington 98195, United States; Center for Urban Waters, Tacoma, Washington 98421, United States;* orcid.org/0000-0001-8107-5968

Zhenyu Tian − *Center for Urban Waters, Tacoma, Washington 98421, United States; Interdisciplinary Arts and Sciences, University of Washington Tacoma, Tacoma, Washington 98421, United States; Department of Chemistry and Chemical Biology, Northeastern University, Boston, Massachusetts 02115, United States;* orcid.org/0000-0002-7491-7028

Melissa Gonzalez − *Center for Urban Waters, Tacoma, Washington 98421, United States*

Craig A. Rideout − *Center for Urban Waters, Tacoma, Washington 98421, United States*

Katherine T. Peter − *Center for Urban Waters, Tacoma, Washington 98421, United States; Interdisciplinary Arts and Sciences, University of Washington Tacoma, Tacoma, Washington 98421, United States;* orcid.org/0000-0001-7379-265X

Complete contact information is available at: https://pubs.acs.org/10.1021/acs.est.2c08690

Notes

The authors declare no competing financial interest.

■ ACKNOWLEDGMENTS

This work was supported by EPA grant #01J18101 and NSF grant #1803240. We also thank Kirk Willard for supporting purchases of some laboratory supplies. We thank the Steve and Sylvia Burges Endowed Presidential Fellowship for financial support to H.N.Z. We thank Dale Whittington at the UW Medicinal Chemistry Mass Spectrometry Center for his help on LC-DAD experiments.

■ REFERENCES

(1) Fairbairn, D. J.; Elliott, S. M.; Kiesling, R. L.; Schoenfuss, H. L.; Ferrey, M. L.; Westerhoff, B. M. Contaminants of Emerging Concern in Urban Stormwater: Spatiotemporal Patterns and Removal by Iron-Enhanced Sand Filters (IESFs). *Water Res.* **2018**, *145*, 332−345.

(2) Richardson, S. D.; Kimura, S. Y. Water Analysis: Emerging Contaminants and Current Issues. *Anal. Chem.* **2020**, *92*, 473−505.

(3) Masoner, J. R.; Kolpin, D. W.; Cozzarelli, I. M.; Barber, L. B.; Burden, D. S.; Foreman, W. T.; Forshay, K. J.; Furlong, E. T.; Groves, J. F.; Hladik, M. L.; Hopton, M. E.; Jaeschke, J. B.; Keefe, S. H.; Krabbenhoft, D. P.; Lowrance, R.; Romanok, K. M.; Rus, D. L.; Selbig, W. R.; Williams, B. H.; Bradley, P. M. Urban Stormwater: An Overlooked Pathway of Extensive Mixed Contaminants to Surface and Groundwaters in the United States. *Environ. Sci. Technol.* **2019**, *53*, 10070−10081.

(4) Hiki, K.; Nakajima, F.; Tobino, T. Causes of Highway Road Dust Toxicity to an Estuarine Amphipod: Evaluating the Effects of Nicotine. *Chemosphere* **2017**, *168*, 1365−1374.

(5) Spromberg, J. A.; Baldwin, D. H.; Damm, S. E.; McIntyre, J. K.; Huff, M.; Sloan, C. A.; Anulacion, B. F.; Davis, J. W.; Scholz, N. L. Coho Salmon Spawner Mortality in Western US Urban Watersheds: Bioinfiltration Prevents Lethal Storm Water Impacts. *J. Appl. Ecol.* **2016**, *53*, 398−407.

(6) Carpenter, C. M. G.; Wong, L. Y. J.; Johnson, C. A.; Helbling, D. E. Fall Creek Monitoring Station: Highly Resolved Temporal Sampling to Prioritize the Identification of Nontarget Micropollutants in a Small Stream. *Environ. Sci. Technol.* **2019**, *53*, 77−87.

(7) Spahr, S.; Teixidó, M.; Sedlak, L.; Luthy, R. Hydrophilic Trace Organic Contaminants in Urban Stormwater: Occurrence, Toxicological Relevance, and the Need to Enhance Green Stormwater Infrastructure. *Environ. Sci. Water Res. Technol.* **2020**, *6*, 15−44.

(8) Tian, Z.; Peter, K. T.; Gipe, A. D.; Zhao, H.; Hou, F.; Wark, D. A.; Khangaonkar, T.; Kolodziej, E. P.; James, C. A. Suspect and Nontarget Screening for Contaminants of Emerging Concern in an Urban Estuary. *Environ. Sci. Technol.* **2020**, *54*, 889−901.

(9) Tian, Z.; Zhao, H.; Peter, K. T.; Gonzalez, M.; Wetzel, J.; Wu, C.; Hu, X.; Prat, J.; Mudrock, E.; Hettinger, R.; Cortina, A. E.; Biswas, R. G.; Kock, F. V. C.; Soong, R.; Jenne, A.; Du, B.; Hou, F.; He, H.; Lundeen, R.; Gilbreath, A.; Sutton, R.; Scholz, N. L.; Davis, J. W.; Dodd, M. C.; Simpson, A.; McIntyre, J. K.; Kolodziej, E. P. A Ubiquitous Tire Rubber−Derived Chemical Induces Acute Mortality in Coho Salmon. *Science* **2021**, *371*, 185−189.

(10) McIntyre, J. K.; Prat, J.; Cameron, J.; Wetzel, J.; Mudrock, E.; Peter, K. T.; Tian, Z.; Mackenzie, C.; Lundin, J.; Stark, J. D.; King, K.; Davis, J. W.; Kolodziej, E. P.; Scholz, N. L. Treading Water: Tire Wear Particle Leachate Recreates an Urban Runoff Mortality Syndrome in Coho but Not Chum Salmon. *Environ. Sci. Technol.* **2021**, *55*, 11767−11774.

(11) Tian, Z.; Gonzalez, M.; Rideout, C. A.; Zhao, H. N.; Hu, X.; Wetzel, J.; Mudrock, E.; James, C. A.; McIntyre, J. K.; Kolodziej, E. P.

6PPD-Quinone: Revised Toxicity Assessment and Quantification with a Commercial Standard. *Environ. Sci. Technol. Lett.* **2022**, *9*, 140−146.
(12) Brinkmann, M.; Montgomery, D.; Selinger, S.; Miller, J. G. P.; Stock, E.; Alcaraz, A. J.; Challis, J. K.; Weber, L.; Janz, D.; Hecker, M.; Wiseman, S. Acute Toxicity of the Tire Rubber-Derived Chemical 6PPD-Quinone to Four Fishes of Commercial, Cultural, and Ecological Importance. *Environ. Sci. Technol. Lett.* **2022**, *9*, 333−338.
(13) Hiki, K.; Yamamoto, H. The Tire-Derived Chemical 6PPD-Quinone is Lethally Toxic to the White-Spotted Char *Salvelinus Leucomaenis Pluvius* but Not to Two Other Salmonid Species. *Environ. Sci. Technol. Lett.* **2022**, *9*, 1050−1055.
(14) Challis, J. K.; Popick, H.; Prajapati, S.; Harder, P.; Giesy, J. P.; McPhedran, K.; Brinkmann, M. Occurrences of Tire Rubber-Derived Contaminants in Cold-Climate Urban Runoff. *Environ. Sci. Technol. Lett.* **2021**, *8*, 961−967.
(15) Gasperi, J.; Le Roux, J.; Deshayes, S.; Ayrault, S.; Bordier, L.; Boudahmane, L.; Budzinski, H.; Caupos, E.; Caubrière, N.; Flanagan, K.; Guillon, M.; Huynh, N.; Labadie, P.; Meffray, L.; Neveu, P.; Partibane, C.; Paupardin, J.; Saad, M.; Varnede, L.; Gromaire, M.-C. Micropollutants in Urban Runoff from Traffic Areas: Target and Non-Target Screening on Four Contrasted Sites. *Water* **2022**, *14*, 394.
(16) Johannessen, C.; Helm, P.; Lashuk, B.; Yargeau, V.; Metcalfe, C. D. The Tire Wear Compounds 6PPD-Quinone and 1,3-Diphenylguanidine in an Urban Watershed. *Arch. Environ. Contam. Toxicol.* **2021**, *82*, 171−179.
(17) Johannessen, C.; Metcalfe, C. D. The Occurrence of Tire Wear Compounds and Their Transformation Products in Municipal Wastewater and Drinking Water Treatment Plants. *Environ. Monit. Assess.* **2022**, *194*, 731.
(18) Monaghan, J.; Jaeger, A.; Agua, A. R.; Stanton, R. S.; Pirrung, M.; Gill, C. G.; Krogh, E. T. A Direct Mass Spectrometry Method for the Rapid Analysis of Ubiquitous Tire-Derived Toxin *N*-(1,3-Dimethylbutyl)-*N*′-Phenyl-*p*-Phenylenediamine Quinone (6-PPDQ). *Environ. Sci. Technol. Lett.* **2021**, *8*, 1051−1056.
(19) Rauert, C.; Charlton, N.; Okoffo, E. D.; Stanton, R. S.; Agua, A. R.; Pirrung, M. C.; Thomas, K. V. Concentrations of Tire Additive Chemicals and Tire Road Wear Particles in an Australian Urban Tributary. *Environ. Sci. Technol.* **2022**, *56*, 2421−2431.
(20) Rauert, C.; Vardy, S.; Daniell, B.; Charlton, N.; Thomas, K. V. Tyre additive chemicals, tyre road wear particles and high production polymers in surface water at 5 urban centres in Queensland, Australia. *Sci. Total Environ.* **2022**, *852*, No. 158468.
(21) Seiwert, B.; Nihemaiti, M.; Troussier, M.; Weyrauch, S.; Reemtsma, T. Abiotic Oxidative Transformation of 6-PPD and 6-PPD Quinone from Tires and Occurrence of Their Products in Snow from Urban Roads and in Municipal Wastewater. *Water Res.* **2022**, *212*, No. 118122.
(22) Johannessen, C.; Helm, P.; Metcalfe, C. D. Detection of Selected Tire Wear Compounds in Urban Receiving Waters. *Environ. Pollut.* **2021**, *287*, No. 117659.
(23) Deng, C.; Huang, J.; Qi, Y.; Chen, D.; Huang, W. Distribution Patterns of Rubber Tire-Related Chemicals with Particle Size in Road and Indoor Parking Lot Dust. *Sci. Total Environ.* **2022**, *844*, No. 157144.
(24) Hiki, K.; Yamamoto, H. Concentration and leachability of N-(1,3-dimethylbutyl)-N′-phenyl-p-phenylenediamine (6PPD) and its quinone transformation product (6PPD-Q) in road dust collected in Tokyo, Japan. *Environ. Pollut.* **2022**, *302*, No. 119082.
(25) Huang, W.; Shi, Y.; Huang, J.; Deng, C.; Tang, S.; Liu, X.; Chen, D. Occurrence of Substituted *p*-Phenylenediamine Antioxidants in Dusts. *Environ. Sci. Technol. Lett.* **2021**, *8*, 381−385.
(26) Klöckner, P.; Seiwert, B.; Weyrauch, S.; Escher, B. I.; Reemtsma, T.; Wagner, S. Comprehensive Characterization of Tire and Road Wear Particles in Highway Tunnel Road Dust by Use of Size and Density Fractionation. *Chemosphere* **2021**, *279*, No. 130530.
(27) Liang, B.; Li, J.; Du, B.; Pan, Z.; Liu, L.-Y.; Zeng, L. E-Waste Recycling Emits Large Quantities of Emerging Aromatic Amines and Organophosphites: A Poorly Recognized Source for Another Two Classes of Synthetic Antioxidants. *Environ. Sci. Technol. Lett.* **2022**, *9*, 625−631.
(28) Johannessen, C.; Saini, A.; Zhang, X.; Harner, T. Air Monitoring of Tire-Derived Chemicals in Global Megacities Using Passive Samplers. *Environ. Pollut.* **2022**, *314*, No. 120206.
(29) Wang, W.; Cao, G.; Zhang, J.; Wu, P.; Chen, Y.; Chen, Z.; Qi, Z.; Li, R.; Dong, C.; Cai, Z. Beyond Substituted *p*-Phenylenediamine Antioxidants: Prevalence of Their Quinone Derivatives in PM2.5. *Environ. Sci. Technol.* **2022**, *56*, 10629−10637.
(30) Wang, W.; Cao, G.; Zhang, J.; Chen, Z.; Dong, C.; Chen, J.; Cai, Z. *p*-Phenylenediamine-Derived Quinones as New Contributors to the Oxidative Potential of Fine Particulate Matter. *Environ. Sci. Technol. Lett.* **2022**, *9*, 712−717.
(31) Zhang, Y.-J.; Xu, T.-T.; Ye, D.-M.; Lin, Z.-Z.; Wang, F.; Guo, Y. Widespread *N*-(1,3-Dimethylbutyl)-*N*′-Phenyl-*p*-Phenylenediamine Quinone in Size-Fractioned Atmospheric Particles and Dust of Different Indoor Environments. *Environ. Sci. Technol. Lett.* **2022**, *9*, 420−425.
(32) Zhang, Y.; Xu, C.; Zhang, W.; Qi, Z.; Song, Y.; Zhu, L.; Dong, C.; Chen, J.; Cai, Z. P-Phenylenediamine Antioxidants in PM2.5: The Underestimated Urban Air Pollutants. *Environ. Sci. Technol.* **2022**, *56*, 6914−6921.
(33) *The Vanderbilt Rubber Handbook*; R.T. Vanderbilt Company, 2010.
(34) Lattimer, R. P.; Hooser, E. R.; Layer, R. W.; Rhee, C. K. Mechanisms of Ozonation of *N*-(1,3-Dimethylbutyl)-*N*′-Phenyl-*p*-Phenylenediamine. *Rubber Chem. Technol.* **1983**, *56*, 431−439.
(35) Huntink, N. M. *Durability of Rubber Products: Development of New Antidegradants for Long-Term Protection*. PhD thesis; University of Twente, 2003.
(36) Klöckner, P.; Seiwert, B.; Wagner, S.; Reemtsma, T. Organic Markers of Tire and Road Wear Particles in Sediments and Soils: Transformation Products of Major Antiozonants as Promising Candidates. *Environ. Sci. Technol.* **2021**, *55*, 11723−11732.
(37) Hu, X.; Zhao, H. N.; Tian, Z.; Peter, K. T.; Dodd, M. C.; Kolodziej, E. P. Transformation Product Formation upon Heterogeneous Ozonation of the Tire Rubber Antioxidant 6PPD (*N*-(1,3-Dimethylbutyl)-*N*′-Phenyl-*p*-Phenylenediamine). *Environ. Sci. Technol. Lett.* **2022**, *9*, 413−419.
(38) Schymanski, E. L.; Jeon, J.; Gulde, R.; Fenner, K.; Ruff, M.; Singer, H. P.; Hollender, J. Identifying Small Molecules via High Resolution Mass Spectrometry: Communicating Confidence. *Environ. Sci. Technol.* **2014**, *48*, 2097−2098.
(39) Peter, K. T.; Tian, Z.; Wu, C.; Lin, P.; White, S.; Du, B.; McIntyre, J. K.; Scholz, N. L.; Kolodziej, E. P. Using High-Resolution Mass Spectrometry to Identify Organic Contaminants Linked to Urban Stormwater Mortality Syndrome in Coho Salmon. *Environ. Sci. Technol.* **2018**, *52*, 10317−10327.
(40) Du, B.; Lofton, J. M.; Peter, K. T.; Gipe, A. D.; James, C. A.; McIntyre, J. K.; Scholz, N. L.; Baker, J. E.; Kolodziej, E. P. Development of Suspect and Non-Target Screening Methods for Detection of Organic Contaminants in Highway Runoff and Fish Tissue with High-Resolution Time-of-Flight Mass Spectrometry. *Environ. Sci. Process. Impacts* **2017**, *19*, 1185−1196.
(41) Zhao, H. N.; Tian, Z.; Kim, K. E.; Wang, R.; Lam, K.; Kolodziej, E. P. Biotransformation of Current-Use Progestin Dienogest and Drospirenone in Laboratory-Scale Activated Sludge Systems Forms High-Yield Products with Altered Endocrine Activity. *Environ. Sci. Technol.* **2021**, *55*, 13869−13880.
(42) *OSPAR Background Document on 4-(Dimethylbutylamino) Diphenylamine (6PPD)*; European Union, 2006.
(43) Cataldo, F.; Faucette, B.; Huang, S.; Ebenezer, W. On the Early Reaction Stages of Ozone with *N*,*N*′-Substituted *p*-Phenylenediamines (6PPD, 77PD) and *N*,*N*′,*N*″-Substituted-1,3,5-Triazine "Durazone®": An Electron Spin Resonance (ESR) and Electronic Absorption Spectroscopy Study. *Polym. Degrad. Stab.* **2015**, *111*, 223−231.
(44) Huang, D.; LaCount, B. J.; Castro, J. M.; Ignatz-Hoover, F. Development of a service-simulating, accelerated aging test method

https://doi.org/10.1021/acs.est.2c08690
Environ. Sci. Technol. 2023, 57, 5621−5632

for exterior tire rubber compounds I. Cyclic aging. *Polym. Degrad. Stab.* **2001**, *74*, 353−362.
(45) Yeh, K.; Ditto, J. C.; Abbatt, J. P. D. Ozonolysis Lifetime of Tetrahydrocannabinol in Thirdhand Cannabis Smoke. *Environ. Sci. Technol. Lett.* **2022**, *9*, 599−603.
(46) Wylie, A. D. L.; Abbatt, J. P. D. Heterogeneous Ozonolysis of Tetrahydrocannabinol: Implications for Thirdhand Cannabis Smoke. *Environ. Sci. Technol.* **2020**, *54*, 14215−14223.
(47) Zhou, S.; Hwang, B. C. H.; Lakey, P. S. J.; Zuend, A.; Abbatt, J. P. D.; Shiraiwa, M. Multiphase Reactivity of Polycyclic Aromatic Hydrocarbons is Driven by Phase Separation and Diffusion Limitations. *Proc. Natl. Acad. Sci. U. S. A.* **2019**, *116*, 11658−11663.
(48) Tian, Z.; Gold, A.; Nakamura, J.; Zhang, Z.; Vila, J.; Singleton, D. R.; Collins, L. B.; Aitken, M. D. Nontarget Analysis Reveals a Bacterial Metabolite of Pyrene Implicated in the Genotoxicity of Contaminated Soil after Bioremediation. *Environ. Sci. Technol.* **2017**, *51*, 7091−7100.
(49) Khan, W.; Wang, Y.-H.; Nanayakkara, N. P. D.; Herath, H. M. T. B.; Catchings, Z.; Khan, S.; Fasinu, P. S.; ElSohly, M. A.; McChesney, J. D.; Khan, I. A.; Chaurasiya, N. D.; Tekwani, B. L.; Walker, L. A. Quantitative Determination of Primaquine-5,6-*ortho*-Quinone and Carboxyprimaquine-5,6-*ortho*-Quinone in Human Erythrocytes by UHPLC-MS/MS. *J. Chromatogr., B* **2021**, *1163*, No. 122510.
(50) McCoull, K. D.; Rindgen, D.; Blair, I. A.; Penning, T. M. Synthesis and Characterization of Polycyclic Aromatic Hydrocarbon *o*-Quinone Depurinating N7-Guanine Adducts. *Chem. Res. Toxicol.* **1999**, *12*, 237−246.
(51) Miao, X.-S.; March, R. E.; Metcalfe, C. D. A Tandem Mass Spectrometric Study of the *N*-Oxides, Quinoline *N*-Oxide, Carbadox, and Olaquindox, Carried out at High Mass Accuracy Using Electrospray Ionization. *Int. J. Mass Spectrom.* **2003**, *230*, 123−133.
(52) Wu, Y.; Farrell, J. T.; Lynn, K.; Euler, D.; Kwei, G.; Hwang, T.-L.; Qin, X.-Z. The Importance of Chromatographic Separation in LC/MS/MS Quantitation of Drugs in Biological Fluids: Detection, Characterization, and Synthesis of a Previously Unknown Low-Level Nitrone Metabolite of a Substance P Antagonist. *Anal. Chem.* **2003**, *75*, 426−434.
(53) Pedersen, C. J. Products of the Photochemical Decomposition of *N*,*N*′-Disubstituted *p*-Quinonediimine-*N*,*N*′-Dioxides. *J. Am. Chem. Soc.* **1957**, *79*, 5014−5019.
(54) Pedersen, C. J. Preparation of *N*, *N*′-Disubstituted *p*-Quinonediimine- *N*,*N*′-Dioxides. *J. Am. Chem. Soc.* **1957**, *79*, 2295−2299.
(55) Mvula, E.; Sonntag, C. Ozonolysis of Phenols in Aqueous Solution. *Org. Biomol. Chem.* **2003**, *1*, 1749−1756.
(56) Tekle-Röttering, A.; von Sonntag, C.; Reisz, E.; Eyser, C. V.; Lutze, H. V.; Türk, J.; Naumov, S.; Schmidt, W.; Schmidt, T. C. Ozonation of Anilines: Kinetics, Stoichiometry, Product Identification and Elucidation of Pathways. *Water Res.* **2016**, *98*, 147−159.
(57) Tentscher, P. R.; Bourgin, M.; von Gunten, U. Ozonation of Para-Substituted Phenolic Compounds Yields p-Benzoquinones, Other Cyclic α,β-Unsaturated Ketones, and Substituted Catechols. *Environ. Sci. Technol.* **2018**, *52*, 4763−4773.
(58) Zoumpouli, G. A.; Zhang, Z.; Wenk, J.; Prasse, C. Aqueous Ozonation of Furans: Kinetics and Transformation Mechanisms Leading to the Formation of α,β-Unsaturated Dicarbonyl Compounds. *Water Res.* **2021**, *203*, No. 117487.
(59) Ramseier, M. K.; Gunten, U. Mechanisms of Phenol Ozonation—Kinetics of Formation of Primary and Secondary Reaction Products. *Ozone: Sci. Eng.* **2009**, *31*, 201−215.
(60) Prasse, C.; Ford, B.; Nomura, D. K.; Sedlak, D. L. Unexpected Transformation of Dissolved Phenols to Toxic Dicarbonyls by Hydroxyl Radicals and UV Light. *Proc. Natl. Acad. Sci. U. S. A.* **2018**, *115*, 2311−2316.
(61) Unice, K. M.; Bare, J. L.; Kreider, M. L.; Panko, J. M. Experimental Methodology for Assessing the Environmental Fate of Organic Chemicals in Polymer Matrices Using Column Leaching Studies and OECD 308 Water/Sediment Systems: Application to Tire and Road Wear Particles. *Sci. Total Environ.* **2015**, *533*, 476−487.
(62) Unice, K. M.; Kreider, M. L.; Panko, J. M. Comparison of Tire and Road Wear Particle Concentrations in Sediment for Watersheds in France, Japan, and the United States by Quantitative Pyrolysis GC/MS Analysis. *Environ. Sci. Technol.* **2013**, *47*, 8138−8147.
(63) Eastman Chemical Company. *Technical Data Sheet for 4-ADPA*. https://www.eastman.com/Pages/ProductHome.aspx?product=71093127, accessed 08, 2021.
(64) World Health Organization *International Agency for Research on Cancer. Monographs on the Evaluation of the Carcinogenic Risk of Chemicals to Humans*; WHO, 1982; Vol. *27*, p. 227.
(65) Zhao, H. N.; Hu, X.; Gonzalez, M.; Rideout, C.; Hobby, G.; Fisher, M.; McCormick, C.; Dodd, M. C.; Kim, K.; Tian, Z.; Kolodziej, E. P. Screening *p*-Phenylenediamine Antioxidants, Their Transformation Products, and Industrial Chemical Additives in Crumb Rubber and Elastomeric Consumer Products. *Environ. Sci. Technol.* **2023**, *57*, 2779.
(66) Avula, B.; Wang, M.; Sagi, S.; Cohen, P. A.; Wang, Y.-H.; Lasonkar, P.; Chittiboyina, A. G.; Feng, W.; Khan, I. A. Identification and Quantification of 1,3-Dimethylbutylamine (DMBA) from Camellia Sinensis Tea Leaves and Dietary Supplements. *J. Pharm. Biomed. Anal.* **2015**, *115*, 159−168.
(67) Cohen, P. A.; Travis, J. C.; Venhuis, B. J. A Synthetic Stimulant Never Tested in Humans, 1,3-Dimethylbutylamine (DMBA), Is Identified in Multiple Dietary Supplements. *Drug Test. Anal.* **2015**, *7*, 83−87.
(68) Cao, G.; Wang, W.; Zhang, J.; Wu, P.; Zhao, X.; Yang, Z.; Hu, D.; Cai, Z. New Evidence of Rubber-Derived Quinones in Water, Air, and Soil. *Environ. Sci. Technol.* **2022**, *56*, 4142−4150.
(69) Hou, F.; Tian, Z.; Peter, K. T.; Wu, C.; Gipe, A. D.; Zhao, H.; Alegria, E. A.; Liu, F.; Kolodziej, E. P. Quantification of Organic Contaminants in Urban Stormwater by Isotope Dilution and Liquid Chromatography-Tandem Mass Spectrometry. *Anal. Bioanal. Chem.* **2019**, *411*, 7791−7806.
(70) Montes, R.; Rodil, R.; Cela, R.; Quintana, J. B. Determination of Persistent and Mobile Organic Contaminants (PMOCs) in Water by Mixed-Mode Liquid Chromatography−Tandem Mass Spectrometry. *Anal. Chem.* **2019**, *91*, 5176−5183.
(71) Elmer, O. C. Tire Cord Adhesives. US4338263A, July 6, 1982.
(72) Johannessen, C.; Helm, P.; Metcalfe, C. D. Runoff of the Tire-Wear Compound, Hexamethoxymethyl-Melamine into Urban Watersheds. *Arch. Environ. Contam. Toxicol.* **2021**, *2*, 162−170.
(73) Alhelou, R.; Seiwert, B.; Reemtsma, T. Hexamethoxymethylmelamine − A Precursor of Persistent and Mobile Contaminants in Municipal Wastewater and the Water Cycle. *Water Res.* **2019**, *165*, No. 114973.
(74) Rauert, C.; Kaserzon, S. L.; Veal, C.; Yeh, R. Y.; Mueller, J. F.; Thomas, K. V. The First Environmental Assessment of Hexa-(Methoxymethyl)Melamine and Co-Occurring Cyclic Amines in Australian Waterways. *Sci. Total Environ.* **2020**, *743*, No. 140834.
(75) Peter, K. T.; Hou, F.; Tian, Z.; Wu, C.; Goehring, M.; Liu, F.; Kolodziej, E. P. More Than a First Flush: Urban Creek Storm Hydrographs Demonstrate Broad Contaminant Pollutographs. *Environ. Sci. Technol.* **2020**, *54*, 6152−6165.
(76) *Federal Highway Administration. Highway Statistics*, 2020. https://www.fhwa.dot.gov/policyinformation/statistics/2020/ (accessed 2023-01-08).
(77) National Centers for Environmental Information. *Annual 2020 National Climate Report*. https://www.ncdc.noaa.gov/sotc/national/202013 (accessed 2023-01-08).
(78) North Carolina Environmental Quality. *Stormwater Design Manual*. https://deq.nc.gov/about/divisions/energy-mineral-and-land-resources/stormwater/stormwater-program/stormwater-design (accessed 2023-01-08).

https://doi.org/10.1021/acs.est.2c08690
Environ. Sci. Technol. 2023, 57, 5621−5632